DE GRUYTER Open Chemistry 2020; 18: 347–356

Research Article

Qiuju Chen, Wenjin Ding*, Tongjiang Peng, and Hongjuan Sun

Synthesis and characterization of calcium carbonate whisker from yellow phosphorus slag

https://doi.org/10.1515/chem-2020-0036
received October 10, 2019; accepted February 21, 2020

Abstract: In this study, a procedure for producing calcium carbonate whisker through yellow phosphorus slag carbonation without adding any crystal control agents was proposed. The influence of process parameters on the crystal phase and morphology of the product was discussed. The content of aragonite in the product was more than 90% under optimal conditions. The whiteness of the product was 97.6%. The diameter of a single particle was about 1.5–3 μm, and the length of a single particle was about 8–40 μm. Various polymorphs and morphologies of $CaCO_3$ could be formed by adjusting the production conditions. The by-products produced during the whole preparation process could also be reused. The whole preparation process of fibrous aragonite from yellow phosphorus slag without using any chemical additives was also proposed. These indicated that the production strategy had a good application prospect.

Keywords: yellow phosphorus slag, calcium carbonate whisker, experimental conditions, growth process

Introduction

Because of its unique physical and chemical properties, precipitated calcium carbonate is widely used in chemical [1–3], food [4], and pharmaceutical industries [5] and in other fields [6,7]. The properties of materials are determined by their structure, and the crystal type and the morphology are the important factors of materials' structure. For example, carbon materials with different polymorphs and morphologies may show different properties [8]. Hence, the structure of the product that plays a crucial role in the preparation process was investigated. Calcium carbonate has three crystal types. They are spherical vaterite, fibrous aragonite, and rhombohedral calcite. Aragonite has a fibrous morphology, and it can be used in the seal and friction material field [9–12]. The market price of calcite and vaterite is much higher than that of aragonite. Therefore, a lot of research studies have been carried out by scholars from China and other countries to produce calcium carbonate whisker [13,14].

Currently, the main methods of preparing calcium carbonate whisker are carbonation, decomposition of calcium bicarbonate, urea hydrolysis, double decomposition, and so on [15–18]. The raw materials used in these methods are mainly pure substances or natural minerals, and chemical additives are usually needed to adjust the morphology of the product during the preparation process. Yellow phosphorus slag is a kind of solid waste produced during the production of yellow phosphorus by the dry process. About 8–10 tons of waste residues may be produced during the production of 1 ton of yellow phosphorus. The main chemical composition of yellow phosphorus slag is amorphous calcium silicate. Hence, the amount of calcium is high in yellow phosphorus slag, and it has good chemical activity. So, it is a good material for producing precipitated calcium carbonate. In China, about 80,00,000 tons of yellow phosphorus slag is produced every year, which can produce 7–10 Mt of calcium carbonate in theory. At present, the slag is mainly used in the field of producing sintered brick [19], glass ceramics [20], and concrete [21]. As far as we know, there are no reports on using yellow phosphorus slag to produce fibrous aragonite.

According to our previous experimental exploration [22], $CaCO_3$ mixed with calcite and aragonite was successfully synthesized. To obtain high-purity calcium carbonate

---

*** Corresponding author: Wenjin Ding,** Key Laboratory of Ministry of Education for Solid Waste Treatment and Resource Recycle, Southwest University of Science and Technology, Mianyang 621010, China; Sichuan Engineering Lab of Non-Metallic Mineral Powder Modification and High-Value Utilization, Southwest University of Science and Technology, Mianyang 621010, China, e-mail: dingwenjin@swust.edu.cn
Qiuju Chen, Tongjiang Peng, Hongjuan Sun: Key Laboratory of Ministry of Education for Solid Waste Treatment and Resource Recycle, Southwest University of Science and Technology, Mianyang 621010, China; Sichuan Engineering Lab of Non-Metallic Mineral Powder Modification and High-Value Utilization, Southwest University of Science and Technology, Mianyang 621010, China

whisker, yellow phosphorus slag was used as a raw material without any chemical additives at low temperature and normal pressure. Using yellow phosphorus slag to prepare aragonite can not only reduce the preparation economic cost but also realize the resource utilization of the slag. The effect of experimental factors such as reaction temperature, Ca^{2+} concentration, ammonia dosage, carbon dioxide velocity, and time on the crystal phase and morphology of the products was systematically discussed in this study. Meanwhile, the whole production process was analyzed, and the economic cost could be reduced by recovering the by-products in theory.

2 Materials and methods

2.1 Materials

The raw material of the slag was obtained from China. The main chemical composition was CaO and SiO_2, and some amount of Fe_2O_3, P_2O_5, and Al_2O_3 was also present (Table 1). The particles were amorphous in nature in the slag (Figure 1a). The microstructure of the slag was granular (Figure 1b). The slag was milled into powder less than 150 μm. The reaction auxiliary was used without further purification, $CaCl_2$, HCl and NH_4OH, and 99.9% CO_2.

2.2 Methods

The whole preparation process was performed according to the experiments of the previous study [22]. During the experiments, the effect of reaction conditions (temperature, concentration of Ca^{2+}, ammonia dosage, CO_2 flow rate, and time) on the preparation process of aragonite was systematically discussed. The concentration of Ca^{2+} in the acid-leaching solution was 1 unit, and it was changed using distilled water and $CaCl_2$. The technological parameters of preparation experiments for aragonite are listed in Table 2.

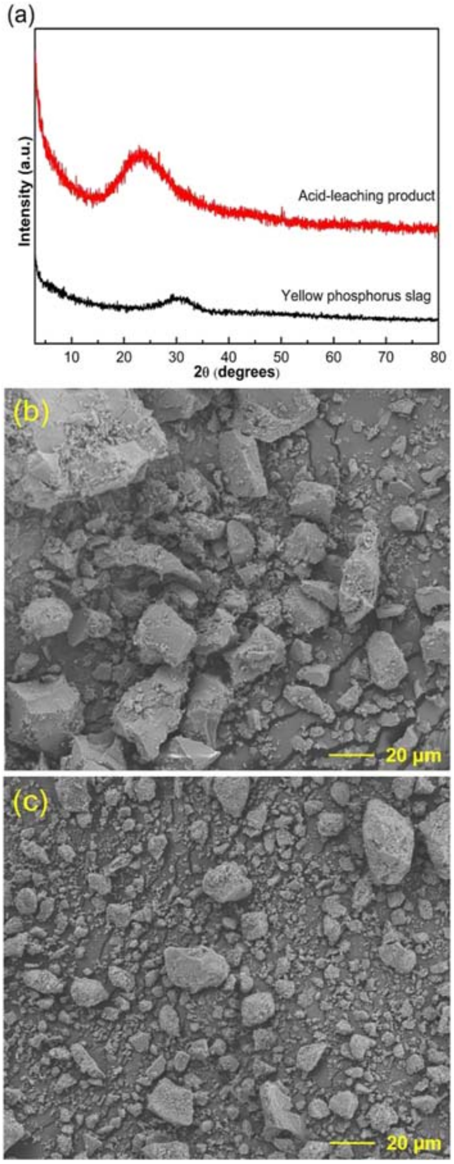

Figure 1: (a) XRD patterns and (b and c) SEM images of yellow phosphorus slag and acid-leaching product.

All the chemical reactions related to the experiments are as follows [23]:

$$CaSiO_3(\text{amorphous}) + 2HCl \rightarrow CaCl_2 + H_2O + SiO_2 \quad (1)$$

Table 1: Composition of yellow phosphorus slag and leaching product (wt%)

Material	CaO	MgO	SiO_2	P_2O_5	Al_2O_3	Fe_2O_3	Others
Yellow phosphorus slag	50.31	2.93	34.70	3.80	3.47	3.12	1.67
Leaching product	0.27	0.05	98.12	0.17	0.31	0.14	0.94

Note: The chemical elements are in the form of oxide.

Table 2: Factors and levels of aragonite preparation experiments

No.	Volume of reaction solution (mL)	Temperature (°C)	Concentration of Ca^{2+}	Ammonia dosage (mL)	CO_2 flow rate (mL/min)	Time (min)	CO_2 purity (%)
1	200	80	4/4	25	100	60	99.9
2	200	100	4/4	25	100	60	99.9
3	200	120	4/4	25	100	60	99.9
4	200	150	4/4	25	100	60	99.9
5	200	100	1/4	25	100	60	99.9
6	200	100	2/4	25	100	60	99.9
7	200	100	3/4	25	100	60	99.9
8	200	100	4/4	25	100	60	99.9
9	200	100	5/4	25	100	60	99.9
10	200	100	6/4	25	100	60	99.9
11	200	100	7/4	25	100	60	99.9
12	200	100	8/4	25	100	60	99.9
13	200	100	4/4	10	100	60	99.9
14	200	100	4/4	15	100	60	99.9
15	200	100	4/4	20	100	60	99.9
16	200	100	4/4	25	100	60	99.9
17	200	100	4/4	30	100	60	99.9
18	200	100	4/4	35	100	60	99.9
19	200	100	4/4	40	100	60	99.9
20	200	100	4/4	25	50	60	99.9
21	200	100	4/4	25	100	60	99.9
22	200	100	4/4	25	150	60	99.9
23	200	100	4/4	25	200	60	99.9
24	200	100	4/4	25	100	30	99.9
25	200	100	4/4	25	100	60	99.9
26	200	100	4/4	25	100	90	99.9
27	200	100	4/4	25	100	120	99.9

$$CaCl_2 + 2NH_4OH \rightarrow Ca(OH)_2 + 2NH_4Cl \tag{2}$$

$$Ca(OH)_2 + CO_2 \rightarrow CaCO_3 + H_2O \tag{3}$$

2.3 Data analysis

The chemical composition of the slag and the products was tested by X-ray fluorescence combined with chemical titration and inductively coupled plasma. The crystal phase of the raw material and the products was determined by the X-ray diffraction (XRD) spectra (an X-ray diffractometer using Cu Kα radiation [$\lambda = 0.15406\,\text{nm}$] at 40 kV, 40 mA with a scanning speed of 0.02 deg/s). The microscopic morphology of the materials was observed using a scanning electron microanalyzer at an accelerating voltage of 5 kV. The specific surface area of leaching product was tested with an Autosorb-1 MP fully automatic specific surface area analyzer (Quantachrome Instruments, USA). The whiteness of the samples was tested using a whiteness meter (HY-BDY).

According to the previous research [24], the mole fractions (mol%) of calcium carbonate with different crystal forms were determined by the following equations, in which I_A^{221}, I_C^{104}, and I_V^{110} are the XRD intensities of the (221) plane of aragonite, the (104) plane of calcite, and the (110) plane of vaterite, respectively.

For a mixture of aragonite and calcite:

$$X_A = \frac{3.157 I_A^{221}}{I_C^{104} + 3.157 I_A^{221}} \tag{4}$$

$$X_C = 1 - X_A \tag{5}$$

For a ternary mixture:

$$X_A = \frac{3.157 I_A^{221}}{I_C^{104} + 3.157 I_A^{221} + 7.691 I_V^{110}} \tag{6}$$

$$X_C = \frac{I_C^{104} \times X_A}{3.157 I_A^{221}} \tag{7}$$

$$X_V = 1.0 - X_A - X_C. \tag{8}$$

Ethical approval: The research conducted is not related to either human or animal use.

3 Results and discussion

3.1 Extraction of calcium from yellow phosphorus slag

The effect of reaction factors on the extraction ratio of calcium was studied with several selected parameters. According to the previous research, the optimal conditions for extracting calcium from yellow phosphorus slag were 3 mol/L, 60°C, 8 mL/g, and 60 min. The main chemical composition of the corresponding reaction product was silicon dioxide. The microscopic morphology of the product was granular, and there were some pores on the surface of the reaction product. The content of silicon dioxide in the reaction product was 98.12%, and the whiteness of the product was 65.4%. The specific surface area of the reaction product was 74.24 m^2/g, which indicated that the reaction product has good reaction reactivity. Therefore, it can be used directly as a filler, and it can also be used as a raw material to produce white carbon black [22].

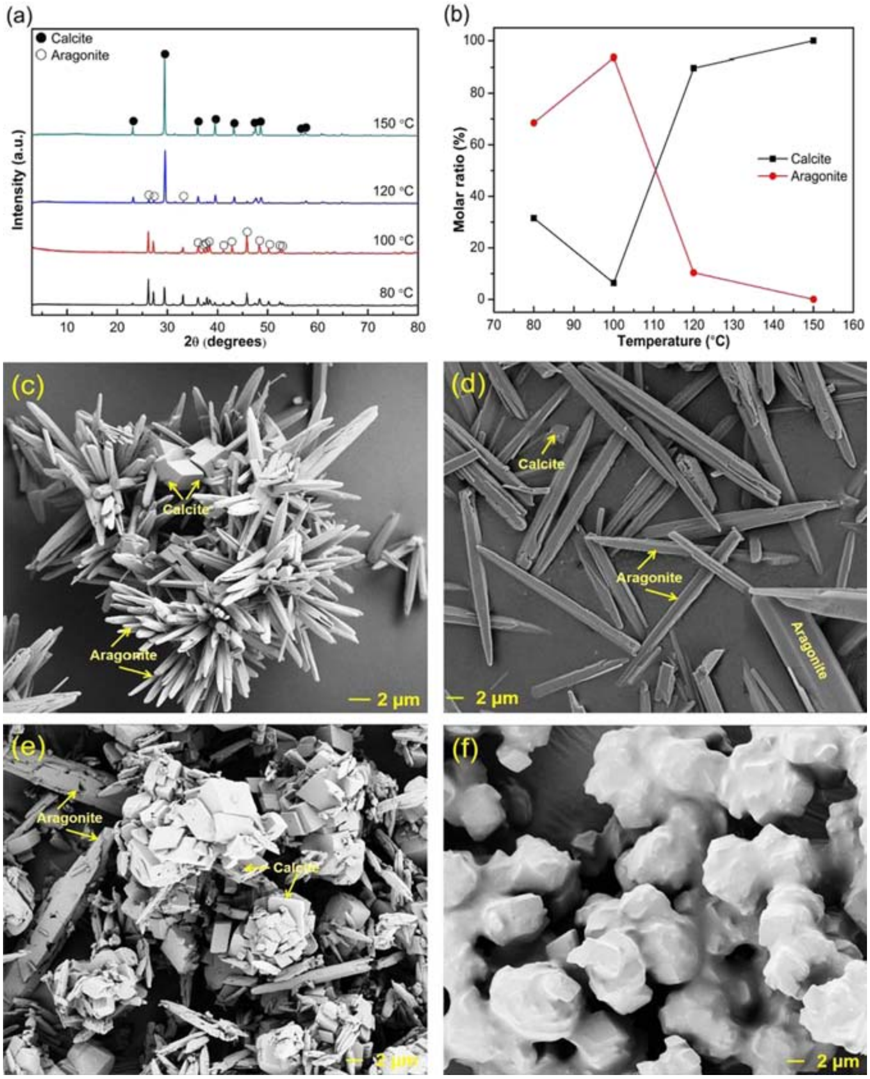

Figure 2: Effect of reaction temperature on crystal phase and morphology: (a) XRD patterns of the product, (b) composition of the products calcite and aragonite, and SEM images of the product at (c) 80°C, (d) 100°C, (e) 120°C, and (f) 150°C.

3.2 Preparation of aragonite

Calcium carbonate has three crystal types. They are spherical vaterite, fibrous aragonite, and rhombohedral calcite. Calcite has the highest thermodynamic stability, aragonite takes second place, and vaterite has the lowest thermodynamic stability [24]. This indicates that the reaction temperature can affect the crystal phase and microscopic morphology of calcium carbonate (Figure 2). Fibrous aragonite mixed with some cubic calcite was synthesized at 80°C (Figure 2a and c). The molar fraction of aragonite and calcite was 68.46% and 31.54%, respectively (Figure 2b). The mole content of aragonite increased to 93.67% and that of calcite reduced

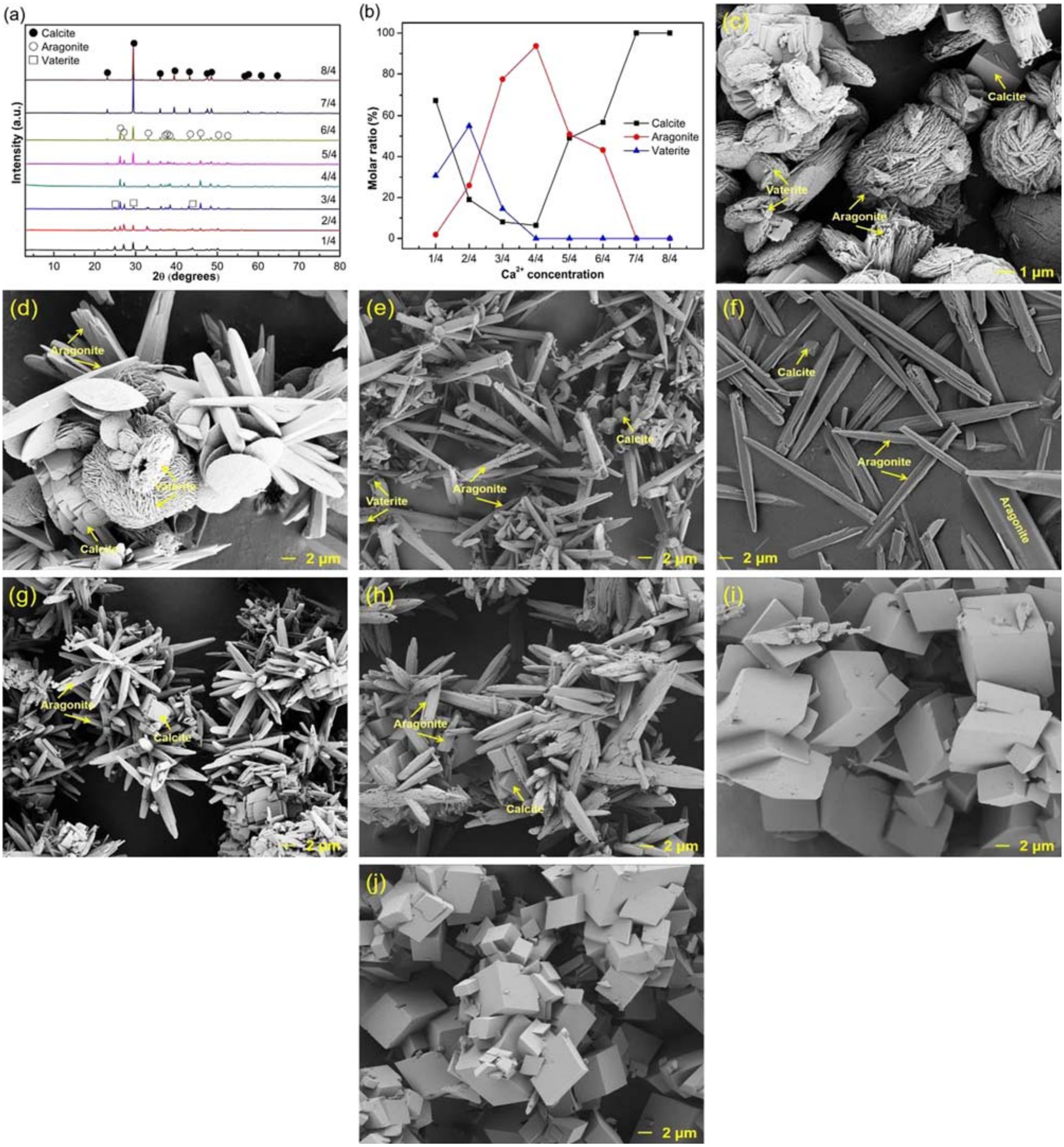

Figure 3: Effect of Ca^{2+} concentration on crystal phase and morphology: (a) XRD patterns of the product, (b) composition of the products calcite, aragonite, and vaterite, and SEM images of the product at (c) 1/4, (d) 2/4, (e) 3/4, (f) 4/4, (g) 5/4, (h) 6/4, (i) 7/4, and (j) 8/4.

correspondingly to 6.33% (Figure 2b) when the reaction temperature was 100°C, and the products were mixture of fibrous aragonite and little cubic calcite (Figure 2a, c and d). This was because the solubility of calcium carbonate in the solution increased gradually, and the solubility of carbon dioxide and calcium hydroxide in the solution decreased with an increase in reaction temperature. Then, calcium carbonate particles were prone to grow along the *c* axis [25]. If the reaction temperature was further increased to 120°C and 150°C, the content of aragonite decreased and that of calcite increased correspondingly. Meanwhile, the mole fraction of aragonite was 10.37% and 0%, and the mole fraction of calcite was 89.63% and 100%, respectively, at reaction temperatures 120°C and 150°C (Figure 2b). Single cubic calcite was obtained at 150°C (Figure 2a and f). This indicated that the increase in temperature is favorable for the transition of calcium carbonate to a more thermodynamically stable crystalline form [24].

Figure 3 shows the effect of Ca^{2+} concentration on the product phase and morphology. The product comprising spherical vaterite, fibrous aragonite, and cubic calcite was prepared when the Ca^{2+} concentration was 1/4 (Figure 3a and c). The molar content was 30.69% for vaterite, 1.9% for aragonite, and 67.41% for calcite (Figure 3b). With the increase in Ca^{2+} concentration from 1/4 to 4/4, the content of calcite and vaterite decreased and the content of aragonite increased (Figure 3b). Some calcite and vaterite transformed into aragonite (Figure 3a). With the increase in Ca^{2+} concentration to 5/4 and 6/4, the crystal phase of vaterite disappeared. The molar content of calcite changed from 49.07% to 56.78%, and the mole

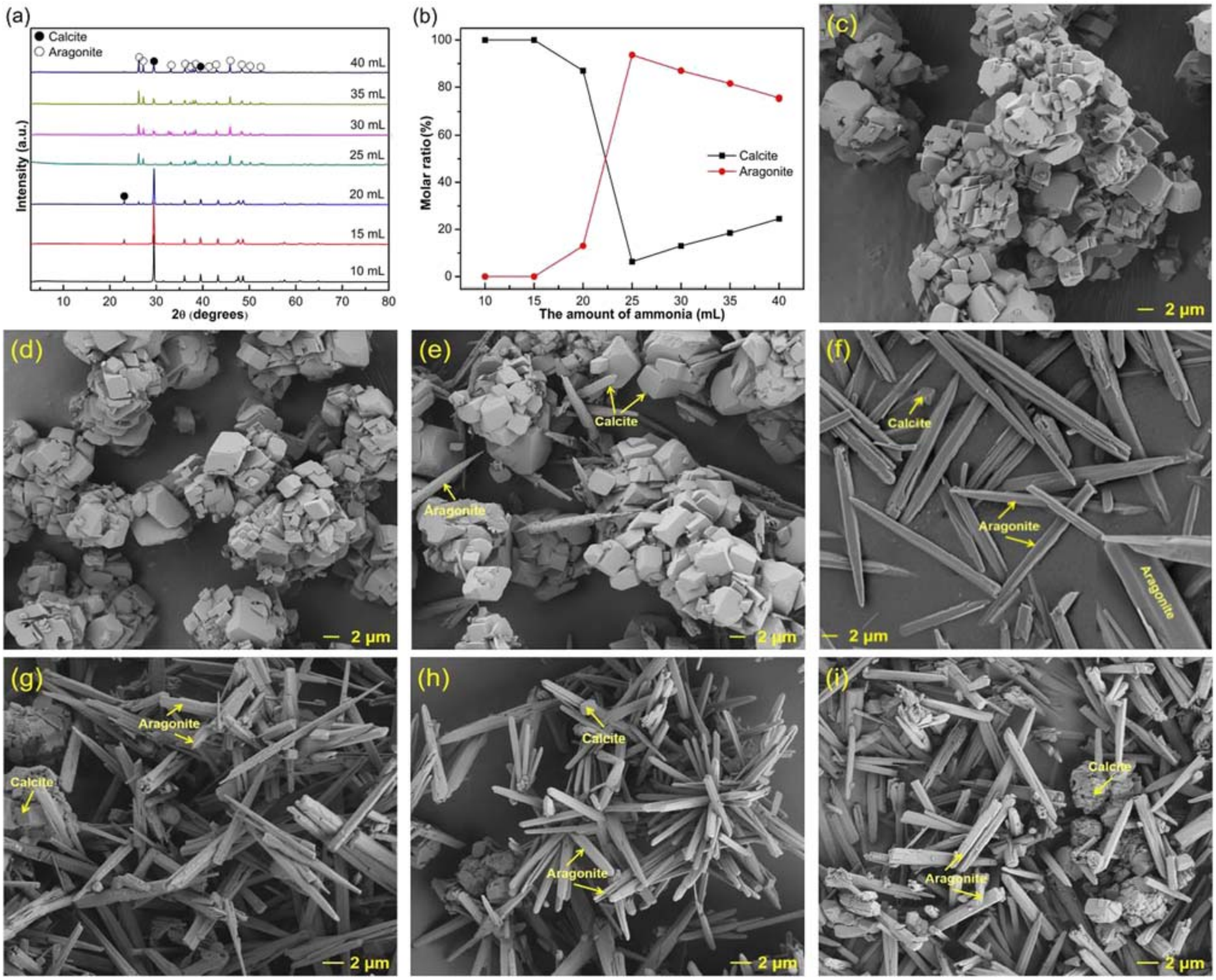

Figure 4: Effect of ammonia dosage on crystal phase and morphology: (a) XRD patterns of the product, (b) composition of the products calcite and aragonite, and SEM images of the product at (c) 10 mL, (d) 15 mL, (e) 20 mL, (f) 25 mL, (g) 30 mL, (h) 35 mL, and (i) 40 mL.

content of aragonite decreased from 50.93% to 43.22% (Figure 3b). If the Ca^{2+} concentration was further increased to 7/4 and 8/4, the phase of the product was calcite with cubic morphology, and there were no other phases (Figure 3a, i and j). Thus, it was beneficial to synthesize vaterite when the concentration of Ca^{2+} was not high. With the addition of calcium chloride, the concentration of Ca^{2+} increased gradually in the solution. Vaterite transformed into thermodynamically metastable aragonite, and aragonite transformed into thermodynamically stable calcite [26,27].

The effect of NH_4OH dosage on product phases is shown in Figure 4. Pure calcite was obtained with 10 and 15 mL ammonia (Figure 4a and c). When the ammonia dosage increased to 25 mL, the mole content of calcite decreased to 6.33% and the mole content of aragonite increased to 93.67% (Figure 4b). The product was composed of fibrous aragonite and little cubic calcite (Figure 4a and d–f). Further increasing the ammonia dosage to 30, 35, and 40 mL, the content of aragonite decreased gradually (Figure 4a and g–i). Then, 25 mL was the optimized ammonia dosage in the system for producing aragonite. The variation trend of content of aragonite was the same among Ca^{2+} concentration, ammonia dosage, and CO_2 flow rate (Figure 5). The optimized CO_2 flow rate was 100 mL/min. The amount of CO_3^{2-} increased per unit time when increasing carbon dioxide velocity. The concentration of Ca^{2+} was constant, and metastable aragonite was first produced, then it gradually transformed into stable calcite with increasing

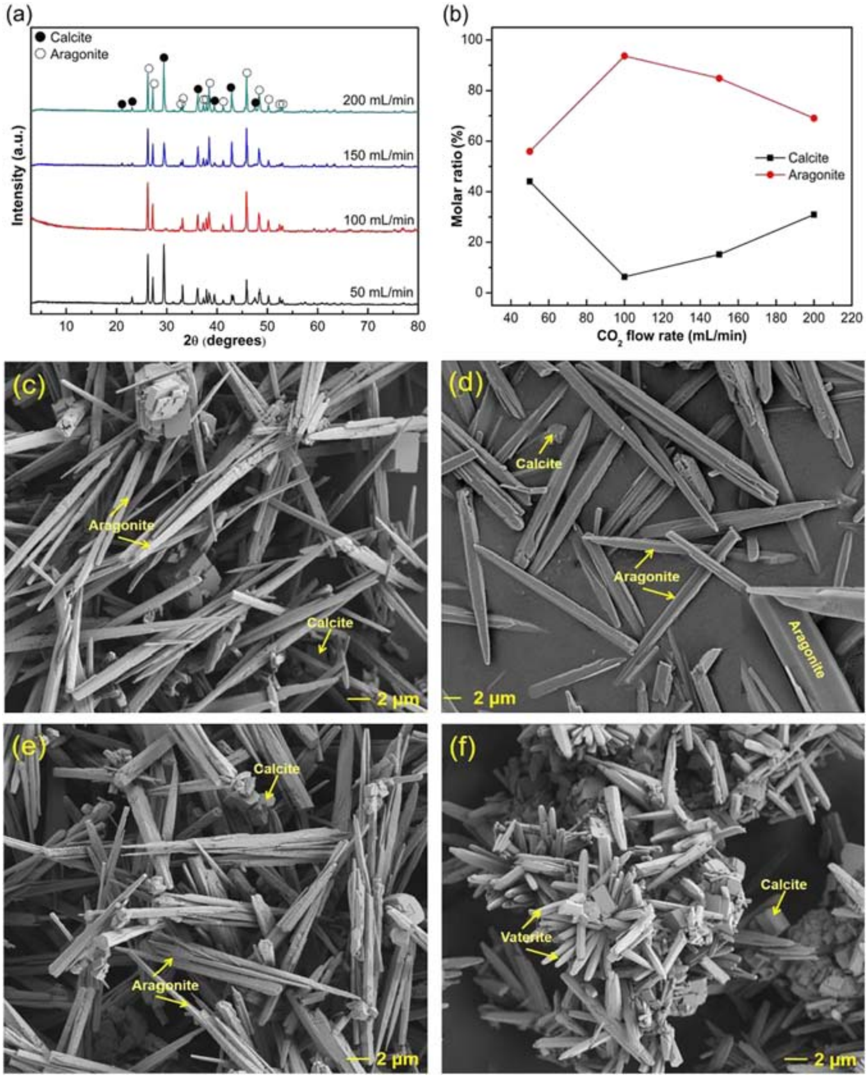

Figure 5: Effect of CO_2 flow rate on crystal phase and morphology: (a) XRD patterns of the product, (b) composition of the products calcite and aragonite, and SEM images of the carbonation product at (c) 50 mL/min, (d) 100 mL/min, (e) 150 mL/min, and (f) 200 mL/min.

amount of CO_3^{2-} [28]. Therefore, increasing carbon dioxide velocity in the reaction system was useful for preparing calcite.

We also discussed the impact of reaction time on the crystal phase of the product (Figure 6). The main crystal phase was fibrous aragonite, and there were also some cubic particles in the product when the reaction time was 30 min (Figure 6a and c). The molar content of aragonite was 64.14%, and the molar content of calcite was 35.86% (Figure 6b). With appropriate prolonging of the reaction time, cubic calcite transformed into fibrous aragonite. The product with more fibrous aragonite was produced for the reaction of 60 min, and the content of aragonite in the product was the highest (Figure 6a, b and d). If the reaction time was further increased to 90 and 120 min, some aragonite transformed into calcite, and the length of the aragonite became shorter (Figure 6a, e and f). The content of aragonite decreased from 93.67% to 49.56% and that of calcite increased correspondingly from 6.33% to 50.44% (Figure 6b). This indicated that the transformation of aragonite to more stable calcite was inevitable when the reaction time was enough, which was the same as the previous research [29,30].

According to the aforementioned research, aragonite was successfully prepared using yellow phosphorus slag as a raw material without any chemical additives. The content of $CaCO_3$ in the product was 99.68%, and the content of aragonite in the product was 93.67%. The whiteness of the product was 97.6%. The aragonite

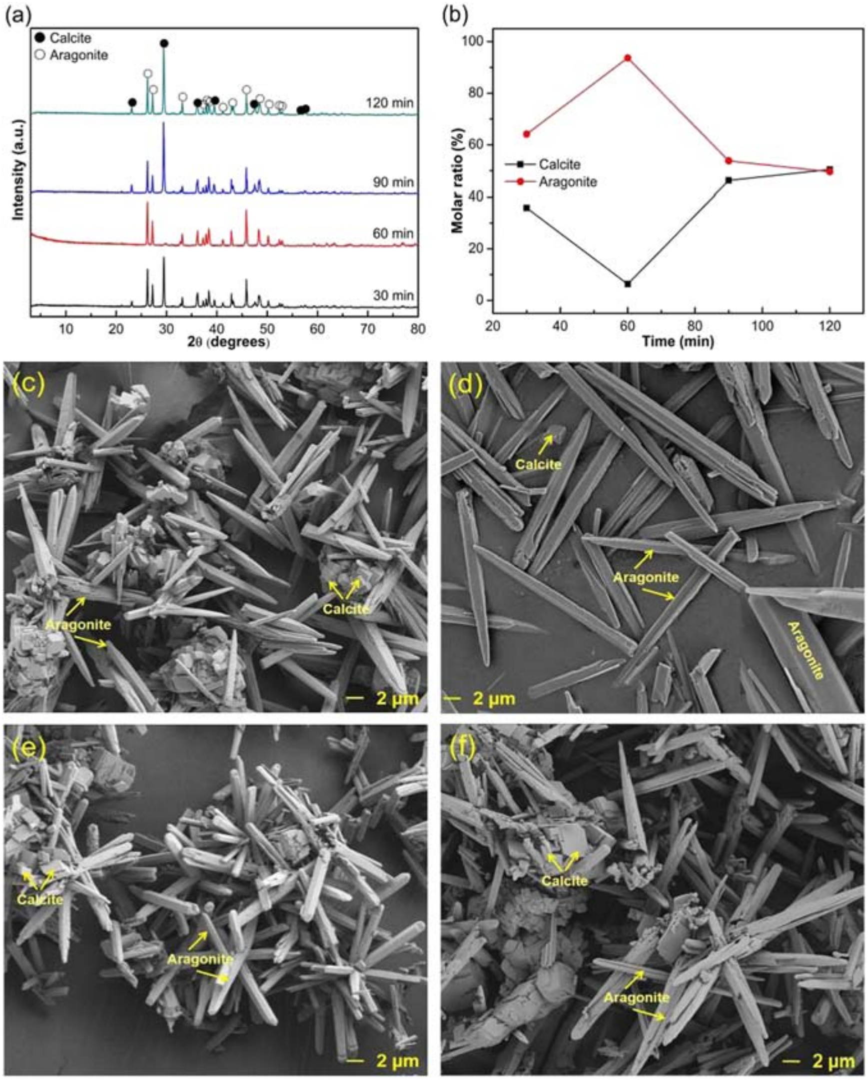

Figure 6: Effect of reaction time on crystal phase and morphology: (a) XRD patterns of the product, (b) composition of the products calcite and aragonite, and SEM images of the product: (c) 30 min, (d) 60 min, (e) 90 min, and (f) 120 min.

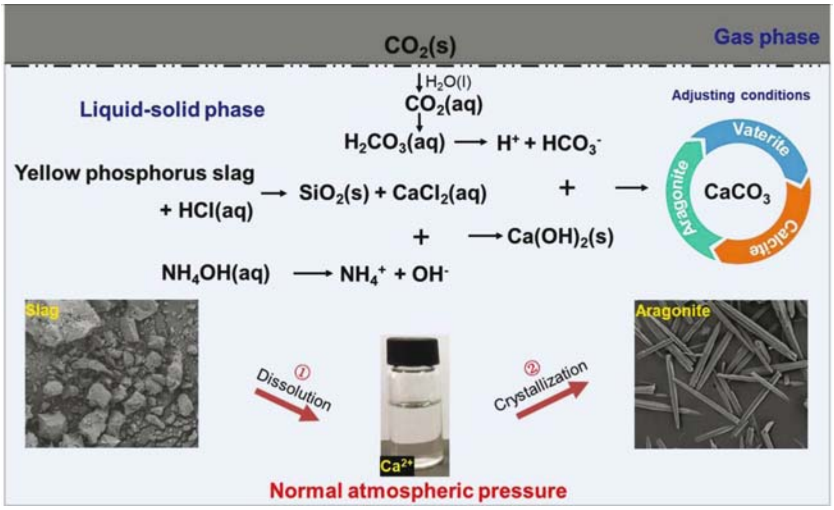

Figure 7: Proposed schematic diagram of yellow phosphorus slag carbonation for aragonite production.

samples had a fibrous morphology, and the surface of the sample was very smooth. The diameter of a single particle was about 1.5–3 μm, and the length of a single particle was about 8–40 μm (Figure 6d). The by-product NH_4Cl can be obtained by evaporating the reaction filtrate, which can reduce the production economic costs. Aragonite samples prepared in the study can be used in packing fields to improve the mechanical strength of composite materials [31] and to replace asbestos for friction and seal materials.

3.3 Crystal growth process

The whole process of aragonite production from yellow phosphorus slag is shown in Figure 7. Yellow phosphorus slag was rich in calcium, which laid a foundation for the preparation of aragonite. First, Ca^{2+} was leached from raw material with the action of hydrochloric acid. After the reaction solution was cooled to 25°C, the pH value of the reaction solution was adjusted to be neutral using ammonium. Meanwhile, ferric hydroxide was precipitated from the solution. Second, calcium hydroxide was formed in the reaction system under the action of ammonium [23]. Third, gaseous CO_2 was dissolved in water to transform $Ca(OH)_2$ to $CaCO_3$ at low temperature and normal pressure. Highly pure aragonite samples can be prepared by adjusting the experimental conditions. During the production process, pure cubic calcite can also be produced. Compared with the previous studies [32,33], no chemical additives were used in the production process. The raw material was industrial solid waste, and the reaction conditions were mild. So, the whole production cost may be much lower than that of the traditional preparation method in theory. The preparation experiment under the optimized conditions will be done in large scale, and the economic cost will be calculated in a follow-up study.

4 Conclusion

In our research, highly pure calcium carbonate whisker was successfully prepared with yellow phosphorus slag as a raw material under the action of HCl and NH_4OH. The technological parameters (temperature, concentration of Ca^{2+}, and ammonia dosage) have an important effect on the crystal type and microscopic morphology of the product. The products with single calcite, mixture of calcite and aragonite, or mixture of calcite, aragonite, and vaterite were all produced without using any chemical additives in the research. The content of aragonite in the product was 93.67% under optimal conditions. The whiteness of the product was 97.6%. The single particle diameter was about 1.5–3 μm, and the length of a single particle was about 8–40 μm. The by-products, including SiO_2 residue and NH_4Cl, could be utilized to reduce the economic cost in the whole production process.

Acknowledgments: This work was supported by the National Key R&D Program of China (2018YFC1802902), the Doctoral Foundation of Southwest University of Science and Technology (17zx7117), and the Longshan Academic Talent Research and Innovation Team Project of SWUST (18lzx401).

Conflict of interest: The authors declare no conflict of interest.

References

[1] He X, Sun H, Zhu M, Yaseen M, Liao D, Cui X, et al. N-Doped porous graphitic carbon with multi-flaky shell hollow structure prepared using a green and ‘useful’ template of $CaCO_3$ for VOC fast adsorption and small peptide enrichment. Chem Commun. 2017;53:3442–5.

[2] Kuo D, Nishimura T, Kajiyama S, Kato T. Bioinspired environmentally friendly amorphous $CaCO_3$-based transparent composites comprising cellulose nanofibers. ACS Omega. 2018;3:12722–9.

[3] Rungpin N, Pavasupree S, Prasassarakich P, Poompradub S. Production of nano-calcium carbonate from shells of the freshwater channeled applesnail, Pomacea canaliculata, by hydrothermal treatment and its application with polyvinyl chloride. Polym Compos. 2015;36:1620–8.

[4] Sun S, Ding H, Hou X, Chen D, Yu S, Zhou H, et al. Effects of organic modifiers on the properties of TiO_2-coated $CaCO_3$ composite pigments prepared by the hydrophobic aggregation of particles. Appl Surf Sci. 2018;456:923–31.

[5] Zhou Y, Li H, Liu J, Xu Y, Wang Y, Ren H, et al. Acetate chitosan with $CaCO_3$ doping form tough hydrogel for hemostasis and wound healing. Polym Adv Technol. 2019;30:143–52.

[6] Lauth V, Maas M, Rezwan K. An evaluation of colloidal and crystalline properties of $CaCO_3$ nanoparticles for biological applications. Mater Sci Eng C. 2017;78:305–14.

[7] Chen F-F, Zhu Y-J, Xiong Z-C, Sun T-W, Shen Y-Q. Highly flexible superhydrophobic and fire-resistant layered inorganic paper. ACS Appl Mater Interfaces. 2016;8:34715–24.

[8] Wang D, Xu L, Nai J, Bai X, Sun T. Morphology-controllable synthesis of nanocarbons and their application in advanced symmetric supercapacitor in ionic liquid electrolyte. Appl Surf Sci. 2019;473:1014–23.

[9] Yang Z-T, Xu W-H, Yin X-C, Qu J-P. Properties and morphology of poly(lactic acid)/calcium carbonate whiskers composites prepared by a vane mixer based on an extensional flow field. J Macromol Sci Part B Phys. 2018;57:418–36.

[10] Ahn J-W, Ramakrishna C, Thenepalli T. A brief review of aragonite precipitated calcium carbonate (PCC) synthesis methods and its applications. Korean Chem Eng Res. 2017;55:443–55.

[11] Cui J-Y, Cai Y-B, Yuan W-J, Lv Z-F, Zhang C, Xu S-A. Preparation of PMMA grafted calcium carbonate whiskers and its reinforcement effect in PVC. Polym Compos. 2017;38:2753–61.

[12] Jing Y, Nai X, Dang L, Zhu D, Wang Y, Dong Y, et al. Reinforcing polypropylene with calcium carbonate of different morphologies and polymorphs. Sci Eng Compos Mater. 2018;25:745–51.

[13] Li M, Lebeau B, Mann S. Synthesis of aragonite nanofilament networks by mesoscale self-assembly and transformation in reverse microemulsions. Adv Mater. 2003;15:2032–35.

[14] Hu Z, Deng Y. Synthesis of needle-like aragonite from calcium chloride and sparingly soluble magnesium carbonate. Powder Technol. 2004;140:10–6.

[15] Ota Y, Inui S, Iwashita T, Kasuga T, Abe Y. Preparation of aragonite whisker. J Am Ceram Soc. 2010;78:1983–4.

[16] Wang L, Sondi I, Matijević E. Preparation of uniform needle-like aragonite particles by homogeneous Precipitation. J Colloid Interface Sci. 1999;218:545–53.

[17] Kong J, Liu C, Yang D, Yan Y, Chen Y, Liu Y, et al. A novel basic matrix protein of Pinctada fucata, PNU9, functions as inhibitor during crystallization of aragonite. CrystEngComm. 2019;21:1250–61.

[18] Jiu LI, Chen H. Calcium carbonate whiskers prepared with magnesium dichloride as crystalline controller. J Chin Ceram Soc. 2005;33:1153–6.

[19] Jiang M, Liu H, Fan X, Wang Z. Predicting gaseous pollution of sintered brick preparation from yellow phosphorus slag. Pol J Environ Stud. 2019;28:1719–25.

[20] Liu H-P, Huang X-F, Ma L-P, Chen D-L, Shang Z-B, Jiang M. Effect of Fe_2O_3 on the crystallization behavior of glass-ceramics produced from naturally cooled yellow phosphorus furnace slag. Int J Miner Metall Mater. 2017;24:316–23.

[21] Chen J-S, Zhao B, Wang X-M, Zhang Q-L, Wang L. Cemented backfilling performance of yellow phosphorus slag. Int J Miner Metall Mater. 2010;17:121–6.

[22] Chen Q, Ding W, Sun H, Peng T. Mineral carbonation of yellow phosphorus slag and characterization of carbonated product. Energy. 2019;188:1–13.

[23] Ding W, Yang H, Ouyang J, Long H. Modified wollastonite sequestrating CO_2 and exploratory application of the carbonation products. RSC Adv. 2016;6:78090–9.

[24] Chen J, Xiang L. Controllable synthesis of calcium carbonate polymorphs at different temperatures. Powder Technol. 2009;189:64–9.

[25] Kitamura M. Controlling factor of polymorphism in crystallization process. J Cryst Growth. 2002;237:2205–14.

[26] Watanabe H, Mizuno Y, Endo T, Wang X, Fuji M, Takahashi M. Effect of initial pH on formation of hollow calcium carbonate particles by continuous CO_2 gas bubbling into $CaCl_2$ aqueous solution. Adv Powder Technol. 2009;20:89–93.

[27] Ding W, Chen Q, Sun H, Peng T. Modified mineral carbonation of phosphogypsum for CO_2 sequestration. J CO2 Util. 2019;34:507–15.

[28] Yong SH, Hadiko G, Fuji M, Takahashi M. Crystallization and transformation of vaterite at controlled pH. J Cryst Growth. 2006;289:269–74.

[29] Rodriguez-Blanco JD, Shaw S, Benning LG. The kinetics and mechanisms of amorphous calcium carbonate (ACC) crystallization to calcite, via vaterite. Nanoscale. 2011;3:265–71.

[30] Ding W, Chen Q, Sun H, Peng T. Modified phosphogypsum sequestrating CO_2 and characteristics of the carbonation product. Energy. 2019;182:224–35.

[31] Xing X, Pei J, Li R, Tan X. Effect and mechanism of calcium carbonate whisker on asphalt binder. Mater Res Express. 2019;6:055306.

[32] Fermani S, Dzakula BN, Reggi M, Falini G, Kralj D. Effects of magnesium and temperature control on aragonite crystal aggregation and morphology. CrystEngComm. 2017;19:2451–5.

[33] Tadier S, Rokidi S, Rey C, Combes C, Koutsoukos PG. Crystal growth of aragonite in the presence of phosphate. J Cryst Growth. 2017;458:44–52.